ISBN: 978-3-95450-204-2 ISSN: 2673-5350 doi:10.18429/JACoW-IBIC2019-TUCO04

# LONGITUDINAL PHASE SPACE RECONSTRUCTION FOR THE HEAVY ION ACCELERATOR HELIAC

S. Lauber*[1,2,4], K. Aulenbacher [1,2,4], W. Barth[1,2], C. Burandt[1,2], F. Dziuba[1,2,4], P. Forck[2], V. Gettmann[1,2], M. Heilmann[2], T. Kürzeder[1,2], J. List[1,2,4], M. Miski-Oglu[1,2], H. Podlech[3], A. Rubin[2], M. Schwarz[3], T. Sieber[2], S. Yaramyshev[2]
[1] Helmholtz Institute Mainz, Mainz, Germany
[2] GSI Helmholtzzentrum für Schwerionenforschung, Darmstadt, Germany
[3] Goethe University, Frankfurt, Germany
[4] Johannes Gutenberg University, Mainz, Germany

*Abstract*

At the GSI Helmholtzzentrum für Schwerionenforschung in Darmstadt, Germany, a prototype cryomodule (Advanced Demonstrator) for the superconducting (SC) continuous wave (CW) Helmholtz Linear Accelerator (HELIAC) is under construction. A transport line, comprising quadrupole lenses, rebuncher cavities, beam correctors and sufficient beam instrumentation has been built to deliver the beam from the GSI 1.4 MeV/u High Charge Injector (HLI) to the Advanced Demonstrator, which offers a test environment for SC CW multigap cavities. In order to achieve proper phase space matching, the beam from the HLI must be characterized in detail. In a dedicated machine experiment the bunch shape has been measured with a non destructive bunch shape monitor (BSM). The BSM offers a sufficient spatial resolution to use it for reconstruction of the beam energy spread. Therefore, different bunch projections were obtained by altering the voltage of two rebunchers. These measurements were combined with dedicated beam dynamics simulations using the particle tracking code DYNAMION. The longitudinal bunch shape and density distribution at the beginning of the matching line could be fully characterized.

## INTRODUCTION

Super Heavy Element (SHE) research performs particle collision experiments with medium to heavy ions on heavy targets to cause fusion evaporation reactions. Extremely small cross-sections make a long beam time crucial the experiments [1, 2]. Whilst the GSI Universal Linear Accelerator (UNILAC) [3–7] is upgraded as an exclusive injector for the Facility for Antiproton and Ion Research (FAIR) [6, 7], a new SC CW heavy ion linear accelerator is built at GSI to keep the SHE research competitive. This project is carried out by GSI and HIM [8, 9] under key support of the GUF [10, 11] and in collaboration with the Moscow Engineering Physics Institute (MEPhI) and the Moscow Institute for Theoretical and Experimental Physics (KI-ITEP) [12, 13]. For different modern facilities worldwide, the operation of CW-Linacs is crucial, as for the Spallation Neutron Source (SNS) in the U.S. [14], or medium energy applications in isotope generation, material science and boron-neutron capture therapy [15]. All these ambitious projects strongly rely on proper beam diagnostics, as minimal beam loss is a key quality to the machines as well as for superconducting multigap cavities [16].

### *Helmholtz Linear Accelerator*

In the future, a new warm injector has to provide a 1.4 MeV/u CW heavy ion beam for the SC HELIAC [17]. It comprises of a Radio Frequency Quadrupole (RFQ) and an Interdigital H-Mode cavity (IH) together with two rebuncher cavities. Four cryomodules with compact SC CH cavities, SC solenoids and SC rebunchers [11] form the SC HELIAC section. Key features of the accelerator are a variable output energy (see Table 1) and the capability to provide for CW operation, while keeping the momentum spread low. The accurate implementation of the beam dynamics design is crucial for the CW-Linac project, as beam losses must be minimized to avoid the degradation of the superconducting cavities. Therefore, robust beam diagnostic methods are required, for the commissioning and routine operation.

The HELIAC stays in line with diverse ambitious Linac projects at GSI, namely the FAIR proton Linac [18], the UNILAC proton beam delivery [19–21], the linear heavy ion decelerator HITRAP (Heavy Ion TRAP) [22] and the LIGHT (Laser Ion Generation, Handling and Transport) facility for laser acceleration of protons and heavy ions [23].

Table 1: HELIAC Design Specifications [17]

| | **Value** |
|---|---|
| Mass/charge | ≤6 |
| Frequency | 216.816 MHz |
| Maximum beam current | 1 mA |
| Injection energy | 1.4 MeV/u |
| Variable output energy | 3.5 MeV/u to 7.3 MeV/u |
| Output energy spread | ±3 keV/u |
| Repetition rate | continuous wave |
| Temperature | 4 K |

### *Demonstrator Environment*

During 2017 and 2018, the novel CH design has been tested and validated in two measurement campaigns, with CH0 being the first of series to be extensively examined [17, 24, 25]. Beam from the injector HLI has been

* s.lauber@gsi.de

ISBN: 978-3-95450-204-2 ISSN: 2673-5350 doi:10.18429/JACoW-IBIC2019-TUCO04

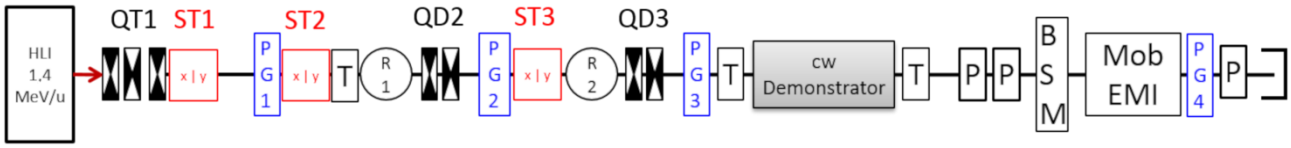


Figure 1: Demonstrator Environment 2018. QT: Quadrupole Triplet, QD: Quadrupole Duplet, R: Rebuncher, x|y: Beam Steerer, PG1-4: SEM-Grid, T: Beam Current Transformer, P: Phase Probe, BSM: Bunch Shape Monitor, EMI: Emittance Meter [17].

delivered to CH0 (installed in a test cryomodule) [26]. The IH-DTL as main part of the HLI is designed with the *KOmbinierte NUll Grad Struktur* (KONUS, in engl.: combined zero degree structure) beam dynamics concept [27, 28], which introduces a non-linear transformation to the bunch shape in the longitudinal phase plane. This arises from using synchronous phases around 0 ° in the most gaps instead of applying typical −30 ° constantly. For longitudinal and transversal matching of the beam to the demonstrator cryomodule, two rebunchers, two quadrupole duplets and a quadrupole triplet were available, as well as three beam steerers for alignment (see Fig. 1). Phase probe sensors were used to determine the beam energy by Time Of Flight (ToF) measurements. The beam profile and position could be measured with Secondary Electron EMission (SEM) grids. For longitudinal bunch shape measurements [29] a Feschenko Monitor [30] was used. Within the demonstrator environment a low beam current was available, which makes space charge effects negligible.

### *Principle of Tomographic Reconstruction*

The distribution $f(x, y)$ (see Fig. 2) has to be recalculated from a set of projections $f_i(x')$. The tomographic reconstruction method also appears in medical diagnostics, where it is used for body imaging. A wide range of reconstruction algorithms already exists for clinical purpose, but they are commonly formulated using linear mappings between $f(x, y)$ and $f_i(x')$ (see Fig. 2), or explicitly base on rotational transformations. For accelerator applications, it is generally not possible to rotate the beam as a solid. Optical elements in the beam line are used to alter the bunch shape, which in most cases is characterized by shearing. When the bunch transformation can be expressed in this way, it is possible to preprocess the data into a sinogram to be used as input for common reconstruction algorithms. In some cases, the bunch transfer is not linear, therefore it is not useful to use sinograms. Suitable algorithms have to be adjusted to this scenarios. The Algebraic Reconstruction Technique (ART) [32] and the Maximum Entropy Tomography Reconstruction (MENT) [33] already have been used for longitudinal phase space reconstruction [33, 34]. A different approach has been investigated for the HELIAC. Instead of using ART or MENT, a Non Negative Least Squares (NNLS) [35] is used to solve the reconstruction problem in the longitudinal phase plane [36].

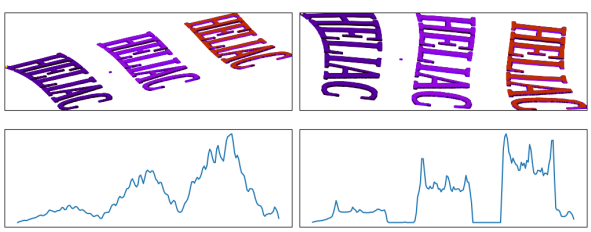


Figure 2: Example of reconstruction setup for a transformation between image and histogram. The observed histograms $f_i(x')$ constrain the shape of the reconstructed object [31].

## METHODS

In order to derive the unknown bunch shape in the longitudinal phase space, different projections must be measured. Therefore, the two rebunchers were used to provide a variety of bunch shapes at the Bunch Shape Monitor (BSM).

### *Bunch Shape Monitor*

The key device for the measurements is the bunch shape monitor Feschenko Monitor. It provides for the longitudinal density distribution of heavy ion beams. With its high resolution of up to 1 degree at 108.408 MHz, it provides for sufficient accuracy to be used for the reconstruction method. The monitor works by placing a metal wire into the beam line and recording the secondary electron emission caused by the beam-wire interaction. Additional electromagnetic lenses improve the signal to noise ratio significantly. A detailed description can be found in [30]. The monitor was located at the end of the line, behind the two rebunchers R1 and R2 as well as behind the cavity (see Fig. 1).

### *Reconstruction*

For the reconstruction, the relation from the input coordinates at the beginning of the beam line (i.e. exit of the HLI) to the coordinates at the Feschenko Monitor must be known. The beamline was described by using the particle tracking code DYNAMION [37], which allows to monitor individual particles along their trajectory. Disposing a grid as input distribution and tracking it through the beamline, the mapping from phase space at the injector HLI to the phase space at the BSM $\vec{f}_i(\vec{x}_{\text{in}})$ could be described for each buncher setting $i$, as well as the projection to the longitudinal spatial axis $A_i(\phi, \vec{X}_{\text{in}})$ for a set of input coordinates $\vec{X}_{\text{in}}$. For a given particle output phase $\phi$, a set of input coordinates $\vec{x}_{\text{in},i}$ exists: $\vec{x}_{\text{in},i}(\phi)$ is ambiguous. In order to

ISBN: 978-3-95450-204-2 ISSN: 2673-5350 doi:10.18429/JACoW-IBIC2019-TUCO04



determine the boundaries, which are used for NNLS reconstruction, the backtracking function $\vec{x}_{\mathrm{in},i}(\phi)$ can be used to select the area of interest for reconstruction. All phases $\phi$, where the signal is below a certain threshold, are selected and tracked back for each histogram. Two areas can be distinguished: with and without signal. By summing up these areas of every histogram, an image can be produced, describing the amount of histograms holding signal/no signal: $N_i(\vec{x}_{\mathrm{in}}) = |\{\phi_i(\vec{x}_{\mathrm{in}})|A(\phi_i(\vec{x}_{in})) \neq 0\}|$.

Furthermore, the mapping $A_i(\phi, \vec{X}_{\mathrm{in}})$ can be expressed in terms of a matrix multiplication $\vec{A}_i = B_i \cdot \vec{X}$ for discrete values $\vec{f}_i(\phi, p)$, which are assembled into $\vec{X}$. With this discretization, also nonlinear mappings can be expressed in terms of $B_i$, which is useful to determine the input distribution $\vec{X}$ with given measurements $\vec{A}_i$. Therefore, all mappings and all measurements can be stacked up into one equation $\vec{A} = B \cdot \vec{X}$. A standart least squared approach would yield negative particle densities. As this is nonphysical, a Non Negative Least Squares approach is chosen, which restricts the result to be $\vec{X} \geq 0$:

$$\begin{aligned} &\text{minimize} \quad f(\vec{X}) = ||B\vec{X} - \vec{A}||_2 \\ &\text{subject to} \quad \vec{X} \geq 0 \end{aligned}$$

The mapping $B$ of the artificial input distribution $\vec{X}$ to all measured histograms $\vec{A}$ should show minimal difference.

## RESULTS

### *Measurements*

All elements in the matching line were adjusted to a state with minimal beam loss for a wide range of rebuncher focusing strengths. 100 BSM-measurements have been conducted with $Ar^{9+}$ beam from the HLI. Combinations of different rebuncher voltages ($R1$,$R2$) were applied, providing for a beam transition from defocusing to overfocusing. Exemplary measurements are presented in Fig. 3. As scheme shown in the histograms, the beam shape is non-symmetrical due to the KONUS beam dynamics of the HLI-IH-DTL. This makes the use of an advanced reconstruction technique necessary, which also considers a non-elliptic bunch shape in the longitudinal phase plane.

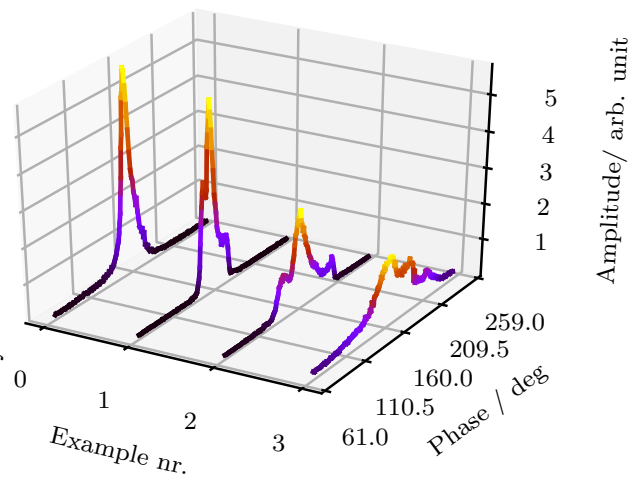


Figure 3: Examples of the bunch shape measurements with the BSM for four different rebuncher settings (108 MHz). The color corresponds to the respective amplitude.

After detailed analysis of the experimental data it was decided to cut 6 % of the signal in order to remove unwanted background. The histograms were mutually realigned to their respective center of mass. In accordance to the algorithm the transmission was assumed to be 100 %.

The measurements with the BSM are presented, such that the head of the bunch is displayed on the right side, the tail on the left (i.e. the beam is divergent). In the following, the phase planes are displayed with the same convention.

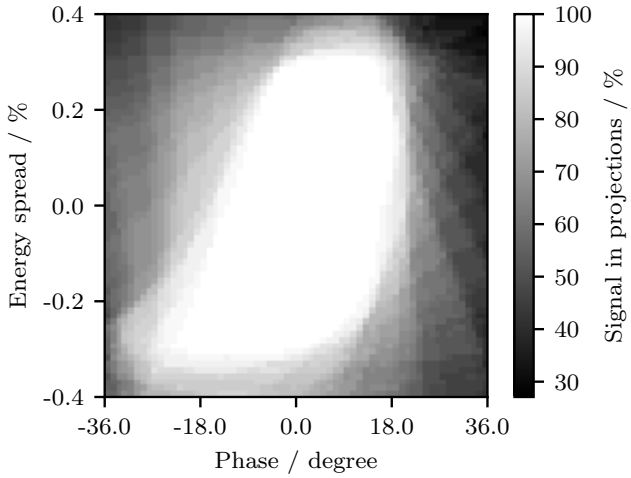


Figure 4: By back projecting the histograms onto the input plane, areas can be marked in which no signal is present and vice versa.

### *Reconstruction*

As described in the previous part, the backprojection of the histograms can be used to determine the area of the bunch in the longitudinal phase space. These limits can be used as boundaries of the NNLS solver. This two step procedure enhances the analysis performance and increases the reliability by using two methods. Because the backprojections overlap from different angles, a signal of 0 % is not derived. For the white area (100 % in Fig. 4) the RMS-emittance could be evaluated for $\epsilon_{\mathrm{RMS}} = 18\,\mathrm{keV/u\,deg}$. This emittance is in good agreement with former simulations of the HLI, which yielded an RMS emittance of 13.5 keV/u deg [38]. The reconstructed emittance are is slightly increased, as the shape reconstruction does not distinguish between low and high signal strengths. By using the limits shown in Fig. 4, the NNLS solver was applied to reconstruct the exact bunch shape and density distribution with the derived boundary values. The NNLS solver reveals a more complicated shape (see Fig. 5). The full emittance is $\epsilon_{\mathrm{RMS}} = 27.3\,\mathrm{keV/u\,deg}$. In the center of the distribution, a remarkably small spot

ISBN: 978-3-95450-204-2 ISSN: 2673-5350 doi:10.18429/JACoW-IBIC2019-TUCO04

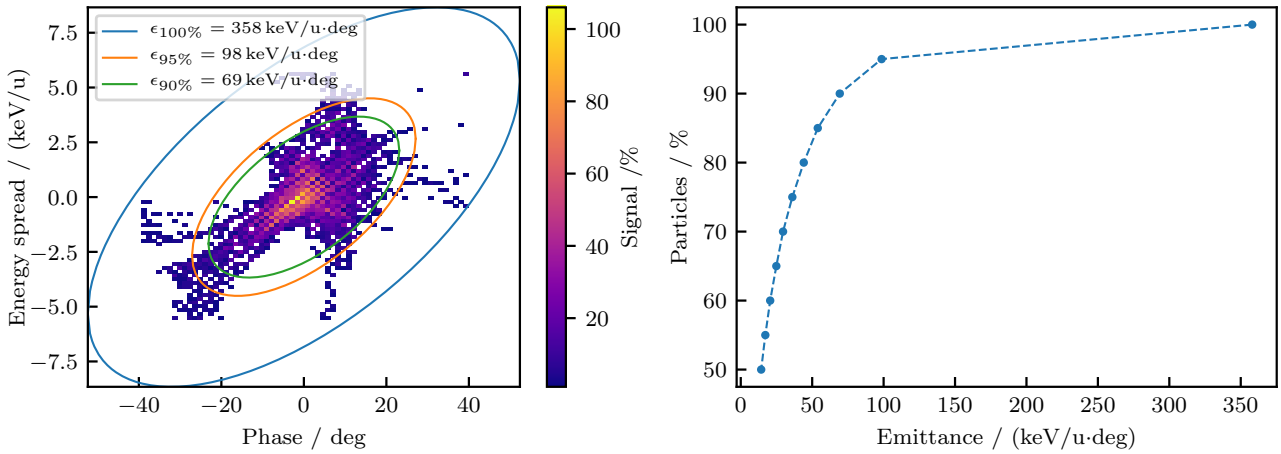


Figure 5: Brilliance analysis of the reconstructed distribution. Samples of the fitted ellipses around a fraction of the density distribution (left) and relation of the emittance on the fraction of particles (right).

with high intensity can be recognized. The analysis of the reconstructed emittance is also presented in Fig. 5. Selected ellipses surrounding a fraction of the particles are displayed. The observed emittance of the bunch is dominated by a marginal percentage of the particles (5 % of the particle distribution), while most of the particles are concentrated in the center. The reconstructed emittance coincide well with the original assumptions for the design of the accelerator. Recently, the BSM was mounted and commissioned at a different position directly at the exit of the injector HLI (i.e. at the reconstruction point) and a dedicated measurement campaign is foreseen to confirm the reconstruction result.

## CONCLUSION & OUTLOOK

Sufficient experimental data has been collected to reconstruct the longitudinal beam characteristics. The shape of the bunch and its density distribution could be reconstructed with the NNLS algorithm from the results of the beam dynamics code DYNAMION. As of now, the matching of the beam to the superconducting continuous wave demonstrator and to the HELIAC can be studied with a higher level of detail to aim for advanced performance of the entire system. It is intended to validate the obtained results by comparing the reconstructed with the measured longitudinal projection at the exit of the HLI, i.e. at the reconstruction point. For the design beam current of 1 mA, additional space charge considerations must be discussed in prospective measurements.

## REFERENCES

[1] M. Block *et al.*, "Direct mass measurements above uranium bridge the gap to the island of stability", *Nature*, vol. 463, pp. 785–788, Feb. 2010. doi:10.1038/nature08774

[2] J. Khuyagbaatar *et al.*, "$^{48}$Ca + $^{249}$Bk Fusion reaction leading to element Z=117: long-lived $\alpha$-decaying $^{270}$Db and discovery of $^{266}$Lr", *Phys. Rev. Lett.*, vol. 112, no. 17, p. 172501, May 2014. doi:10.1103/PhysRevLett.112.172501

[3] W. Barth *et al.*, "U$^{28+}$ intensity record applying a $H_2$ gas stripper cell", *Phys. Rev. ST Accel. Beams*, vol 18, p. 040101, Apr. 2015. doi:10.1103/PhysRevSTAB.18.040101

[4] A. Adonin *et al.*, "Beam brilliance investigation of high current ion beams at GSI heavy ion accelerator facility", *Rev. Sci. Instrum.*, vol. 85, p. 02A727, Apr. 2014. doi:10.1063/1.4833931

[5] S. Yaramyshev *et al.*, "Virtual charge state separator as an advanced tool coupling measurements and simulations", *Phys. Rev. ST Accel. Beams*, vol. 18, p. 050103, May 2015. doi:10.1103/PhysRevSTAB.18.050103

[6] W. Barth *et al.*, "High brilliance uranium beams for the GSI FAIR", *Phys. Rev. ST Accel. Beams*, vol. 20, p. 050101, May 2017. doi:10.1103/PhysRevAccelBeams.20.050101

[7] W. Barth *et al.*, "Upgrade program of the high current heavy ion UNILAC as an injector for FAIR", *Nucl. Instr. Meth. Phys. Res. Sect. A*, vol. 577, no. 1-2, pp. 211–214, Jul. 2007. doi:10.1016/j.nima.2007.02.054

[8] W. Barth *et al.*, "Superconducting CH-Cavity heavy ion beam testing at GSI", *J. Phys. Conf. Ser.*, vol. 1067, p. 052007, Sep. 2018. doi:10.1088/1742-6596/1067/5/052007

[9] F. Dziuba *et al.*, "First cold tests of the superconducting CW demonstrator at GSI", in *Proc. RuPAC'16*, Saint Petersburg, Russia, Nov. 2016, pp. 84–86. doi:10.18429/JACoW-RUPAC2016-WECBMH01

[10] H. Podlech *et al.*, "Superconducting CH structure", *Phys. Rev. ST Accel. Beams*, vol. 10, no. 8, p. 080101, Aug. 2007. doi:10.1103/PhysRevSTAB.10.080101

[11] M. Schwarz *et al.*, "Beam dynamics simulations for the new superconducting CW heavy ion Linac at GSI", *J. Phys.: Conf. Ser.*, vol. 1067, p. 052006, Oct. 2018. doi:10.1088/1742-6596/1067/5/052006

[12] M. Gusarova *et al.*, "Design of the two-gap superconducting re-buncher", *J. Phys.: Conf. Ser.*, vol. 1067, p. 082005, Oct. 2018. doi:10.1088/1742-6596/1067/8/082005

[13] K. Taletskiy *et al.*, "Comparative study of low beta multi-gap superconducting bunchers", *J. Phys.: Conf. Ser.*, vol. 1067, p. 082006, Oct. 2018. doi:10.1088/1742-6596/1067/8/082006

ISBN: 978-3-95450-204-2 ISSN: 2673-5350 doi:10.18429/JACoW-IBIC2019-TUCO04



[14] S.M. Polozov and A.D. Fertman, "High-energy proton beam accelerators for subcritical nuclear reactors", *At. Energ.*, vol. 113, no. 3, pp. 192–200, Jan. 2013. doi:10.1007/s10512-012-9616-4

[15] Zhi-Jun Wang *et al.*, "Beam commissioning for a superconducting proton Linac", *Phys. Rev. Accel. Beams*, vol 19, p. 120101, Dec. 2016. doi:10.1103/PhysRevAccelBeams.19.120101

[16] R. Laxdal *et al.*, "Recent progress in the superconducting RF Program at TRIUMF/ISAC", *Physica C: Superconductivity* vol. 441, no. 1-2, pp. 13, Jul. 2006. doi:10.1016/j.physc.2006.03.096

[17] W. Barth *et al.*, "First heavy ion beam tests with a superconducting multigap CH cavity", *Phys. Rev. Accel. Beams*, vol. 21, no. 2, p. 020102, Feb. 2018. doi:10.1103/PhysRevAccelBeams.21.020102

[18] U. Ratzinger *et al.*, "The 70 MeV p-injector design for FAIR", *AIP Conf. Proc.*, Vol. 773, pp 249-253, 2005. doi:10.1063/1.1949539

[19] W. Barth *et al.*, "Heavy ion Linac as a high current proton beam injector", *Phys. Rev. ST Accel. Beams*, vol. 18, p. 050102, Sep. 2015. doi:10.1103/PhysRevSTAB.18.050102

[20] A. Adonin *et al.*, "Production of high current proton beams using complex H-rich molecules at GSI", *Rev. Sci. Instrum.*, vol. 87, pp. 02B709, 2016. doi:10.1063/1.4934620

[21] P. Forck, "Minimal invasive beam profile monitors for high intense hadron beams", in *Proc. IPAC'10*, Kyoto, Japan, May 2010, paper TUZMH01, pp. 1261–1265.

[22] F. Herfurth *et al.*, "The HITRAP facility for slow highly charged ions", *Physica Scripta*, vol. 2015, no. T166, pp. 014065, Nov. 2015. doi:10.1088/0031-8949/2015/t166/014065

[23] S. Busold *et al.*, "Shaping laser accelerated ions for future applications - The LIGHT collaboration", *Nucl. Instrum. Meth. Phys. Res. Sect. A*, vol. 740, pp. 94-98, Mar. 2014. doi:10.1016/j.nima.2013.10.025

[24] S. Yaramyshev *et al.*, "Advanced approach for beam matching along the multi-cavity SC CW Linac at GSI", *J. Phys. Conf. Ser.*, vol. 1067, p. 052005, Sep. 2018. doi:10.1088/1742-6596/1067/5/052005

[25] S. Minaev *et al.*, "Superconducting, energy variable heavy ion Linac with constant $\beta$, multicell cavities of CH-type", *Phys. Rev. ST Accel. Beams*, vol. 12, p. 120101, Dec. 2009. doi:10.1103/PhysRevSTAB.12.120101

[26] P. Gerhard *et al.*, "Commissioning of a new CW radio frequency quadrupole at GSI", in *Proc. IPAC'10*, Kyoto, Japan, May 2010, paper MOPD028, pp. 741–743.

[27] R. Tiede, U. Ratzinger, H. Podlech, C. Zhang, and G. Clemente, "Konus beam dynamics designs using H-mode cavities", in *Proc. HB'08*, Nashville, TN, USA, Aug. 2008, paper WGB11, pp. 223–230.

[28] R. Tiede *et al.*, "LORASR code development", in *Proc. EPAC'06*, Edinburgh, Scotland, 2006, paper WEPCH118, pp. 2194–2196.

[29] T. Sieber *et al.*, "Bunch shape measurements at the GSI CW-Linac prototype", in *Proc. IPAC'18*, Vancouver, Canada, 2018, pp. 2091-2094. doi:10.18429/JACoW-IPAC2018-WEPAK006

[30] A. V. Feschenko, "Methods and instrumentation for bunch shape measurements", in *Proc. PAC'01*, Chicago, IL, USA, Jun. 2001, paper ROAB002, pp. 517-521.

[31] S. Lauber *et al.*, "Reconstruction of the Longitudinal Phase Portrait for the SC CW Heavy Ion HELIAC at GSI", in *Proc. IPAC'19*, Melbourne, Australia, May 2019, pp. 898–901. doi:10.18429/JACoW-IPAC2019-MOPTS024

[32] R. Gordon, R. Bender, and G. T. Herman, "Algebraic Reconstruction Techniques (ART) for three-dimensional electron microscopy and X-ray photography", *Journal of Theoretical Biology*, vol. 29, no. 3, pp. 471-476, Dec. 1970. doi:10.1016/0022-5193(70)90109-8

[33] K. M. Hock *et al.*, "Beam tomography research at Daresbury Laboratory", *Nucl. Instr. Meth. Phys. Res. Sect. A*, vol. 753, no. 1, pp. 38-55, Jul. 2014. doi:10.1016/j.nima.2014.03.050

[34] D. Malyutin *et al.*, "Longitudinal phase space tomography using a booster cavity at PITZ", *Nucl. Instr. Meth. Phys. Res. Sect. A*, vol. 871, no. 1, Nov. 2017, pp. 105-112. doi:10.1016/j.nima.2017.07.043

[35] C. L. Lawson and R. J. Hanson, *Solving least squares problems*. Philadelphia, PA, USA: Society for Industrial and Applied Mathematics, 1987. doi:10.1137/1.9781611971217

[36] J. Lallement *et al.*, "Linac4 transverse and longitudinal emittance reconstruction in the presence of space charge", in *Proc. LINAC'14*, Geneva, Switzerland, Aug.-Sep. 2014, paper THPP033, pp. 913–915.

[37] S. Yaramyshev *et al.*, "Development of the versatile multi-particle code DYNAMION", *Nucl. Instrum. Meth. Phys. Res. Sect. A*, vol. 558, no. 1, p. 90-95, Mar. 2006. doi:10.1016/j.nima.2005.11.018

[38] U. Ratzinger, "Effiziente Hochfrequenz-Linearbeschleuniger für leichte und schwere Ionen", Habilitation, Phys. Dept., Goethe University, Frankfurt am Main, Germany, 1998.